AJG

Article

National Scale Seagrass Mapping in Vietnam from 1985 to 2019 Using Landsat Images

Xuan Truong Trinh* and Wataru Takeuchi

Institute of Industrial Science, The University of Tokyo, Tokyo, Japan

*Corresponding author: X. T. Trinh < xuantruongtrinh93@g.ecc.u-tokyo.ac.jp>

Received: November 29, 2022; Accepted: March 15, 2023; Published: April 30, 2023

Abstract

Despite their ecological importance, seagrass beds in Vietnam have been subject to rapid decline due to coastal development. While there have been attempts to monitor seagrass beds at individual sites in Vietnam in the past, these studies have been limited in their ability to provide a comprehensive, spatially explicit, and temporally consistent understanding of the extent and distribution of these habitats across the entire nation. To address this issue, the research utilized Landsat imagery spanning a period of over 30 years to provide a spatially explicit and continuous inventory of seagrass beds and quantify land cover changes that have led to seagrass loss. The methodology of the study involved several steps. Firstly, Landsat images over the coastline of Vietnam between 1985 and 2019 were filtered to minimize cloud contamination. Secondly, the selected images were preprocessed to reduce the effects of the water column using Hedley's sun glint correction and Matsunaga's Bottom Index. These preprocessed images were then classified on a scene-by-scene basis using the Random Forest classifier and composited over each five-year period to produce distribution maps. Finally, the distribution maps over time were compared to reveal changes in seagrass distribution. The results of the study indicate that a total of 36,185 ha of seagrass beds in Vietnam were mapped before 1990, but only 17,081 ha remained after 2015. Most meadows lost 40-85% of their area, mainly due to land reclamation. The overall accuracies ranged from 75.8% to 90.4%, while producer's and consumer's accuracy for seagrass ranged from 40.8% to 77.9% and 37.1% to 73.4%, respectively.

Keywords: blue carbon ecosystem; Google Earth Engine; marine habitat.; seagrass mapping; land use land cover change

1. Introduction

Seagrasses are marine flowering plants that inhabit various coastal areas around the world. With their fast growth rate and extensive root networks, seagrass meadows play vital roles in preventing coastal erosion, supporting fisheries, improving water quality, and mitigating climate change (Unsworth et al., 2019). In fact, the carbon burial rate of seagrass beds per hectare is 35 times higher than that of terrestrial (Duarte et al., 2010; Fourqurean et al., 2012; McLeod et al., 2011). Despite their significant environmental importance, seagrass distribution is decreasing rapidly, with an estimated 7% loss per year globally (Waycott et al., 2009). This loss leads to the decline of ecosystem services and the release of carbon sequestered in seagrass beds back into the atmosphere. It is therefore critical to monitor seagrass distribution and prevent further losses. However, there are still significant uncertainties in seagrass monitoring, particularly in the Tropical Indo-Pacific region (Unsworth et al. 2019; Sudo et al. 2021). These uncertainties hinder the accurate quantification of seagrass ecosystems and their contributions to global processes such as carbon sequestration.

However, there are gaps in seagrass monitoring in tropical waters, particularly in the Indo-Pacific region. With 157.5 km^2 of seagrass and the fourth largest seagrass bed area in Southeast Asia, Vietnam is home to 4.3% of the total seagrass area and 14 species, making it the fourth most diverse in the region (Sudo et al., 2021). The seagrass ecosystem services in Vietnam are valued at 72 million dollars, largely due to their role in the fishery (Nguyen, 2013). Despite their importance, seagrass in Vietnam is decreasing rapidly. An estimated 45.4% of the monitored seagrass area in Vietnam has been lost, between 1997 and 2009 (Nguyen, 2013). Some seagrass beds, such as those in Gia Luna, Giang Ninh. have completely disappeared, going from 500 hectares before 1995 to 0 hectares after 2003. Monitoring of seagrass in Vietnam has largely relied on limited field surveys, leading to uncertainty in its spatial and temporal patterns. (Nguyen, 2013).

Satellite- and airborne-based remote sensing has been widely recognized as an effective and cost-efficient method for monitoring seagrass (Hossain et al., 2015; Hossain and Hashim, 2019; T. D. Pham et al., 2019). Multiple techniques have been developed to enhance the reflectance signal of benthic cover impacted by the water ccolumn (Lyzenga, 1978; Lyzenga, 1981; Matsunaga, Hoyano, and Mizukami, 2000; Sagawa et al., 2010; J. D. Hedley, Harborne, and Mumby, 2005). Classification techniques have also been refined and have focused on improving accuracy, increasing long-term coverage and detailed temporal resolution and expanding the spatial coverage of mapping (Lyons, Phinn, and Roelfsema, 2011; Phinn et al., 2018; Lyons, Phinn, and Roelfsema, 2010; Lyons, Roelfsema, and Phinn, 2013; Roelfsema et al., 2013; Traganos and Reinartz, 2018; Traganos et al., 2018; Topouzelis et al., 2018). In addition, there have been efforts to map more detailed indicators of seagrass meadows, such as above-ground biomass and density cover (Roelfsema et al., 2014; Misbari and Hashim, 2016; Hedley et al., 2017; Sani and Hashim, 2019). These technical advances provide the foundation for using remote sensing images to monitor seagrass distribution.

Meta-studies have attempted to provide a comprehensive overview of seagrass beds in Vietnam by collecting different studies of individual sites in Vietnam using remote sensing and field surveys (Cao et al., 2012; Sudo et al., 2021). While these collections of studies are useful for understanding local changes at specific sites, they may contain different methodologies, which limits the comparability of results. To produce comprehensive monitoring across the entire coastline, remote sensing has significant potential due to its coverage and repeatability.

Remote sensing-based studies have been conducted for seagrass in Vietnam at individual sites, such as multitemporal change detection of seagrass beds using Landsat TM, ETM+, and OLI imagery in Cam Ranh Bay, Van Phong Bay, and Ninh Hai (Vo et al., 2020; Quang et al., 2017; Lau, Chen, and Phuoc, 2013; Hoang, Luong, and Ho, 2020; Cao, Dam, and Do, 2005; Cao et al., 2012; Cao, Dam, and Tran, 2019). However, there has been no study that covers both national spatial coverage and a decadal time series for Vietnam or other Southeast Asian countries. This has been challenging, especially in tropical coastal waters, due to the varying water quality, which limits the consistent monitoring of a wide area (Hossain et al., 2019). This gap hinders the development of a national conservation strategy, which requires understanding of the spatial and temporal patterns of nationwide seagrass distribution using a consistent methodology.

This research aims to address the lack of a comprehensive monitoring framework for seagrass in Vietnam by establishing a cloud computing-based framework for national scale seagrass monitoring and analyzing the spatial and temporal patterns of seagrass distribution changes in Vietnam over a 30-year period (1985-2019). By examining seagrass distribution at this spatial and temporal scale, we can gain a better understanding of how seagrass distribution has changed along Vietnam's entire coastline and lay the foundation for studying the nation's seagrass biomass inventory and improving conservation policy. This framework may also be beneficial to other countries with similar coastal conditions.

2. Study Area and Materials

2.1 Study Area

Vietnam boasts a diverse array of coastal environments, with a 1,650 km long coastline. The country is home to 14 distinct seagrass species, including *Enhalus acoroides, Thalassia hemprichii, Halophila ovalis, Halodule uninervis*, and *Zostera japonica*. The South-central coast and Phu Quoc Islands exhibit the highest level of seagrass species diversity, with 9 species present. Conversely, the North-central coast and Northeastern regions of Vietnam typically have a lower diversity of seagrass species, which are primarily found near river mouths or lagoons and consist of only two species: *Halophila ovalis* and *Zostera japonica*. Vietnam's climate is characterized by two main seasons: dry and rainy. Seagrass growth is most robust during the dry months, as the longer hours of sunlight, lower turbidity, and higher salinity levels promote growth. Conversely, during the rainy season, increased precipitation leads to increased discharge from rivers, resulting in elevated turbidity and decreased salinity levels in coastal waters, particularly in closed bays and lagoons. These conditions are unfavorable for seagrass growth, causing a slowdown or die-off. As the rainy season ends, waters recover their clarity and salinity, allowing for seagrass to regrow or grow from deposited seeds. However, this phenomenon is less pronounced in exposed coastal areas without nearby river discharge, as turbidity and salinity levels do not fluctuate significantly (Nguyen, 2004; Nguyen, 2013). The months when rainy season occurs differ among the regions in Vietnam, as detailed in Table S1.

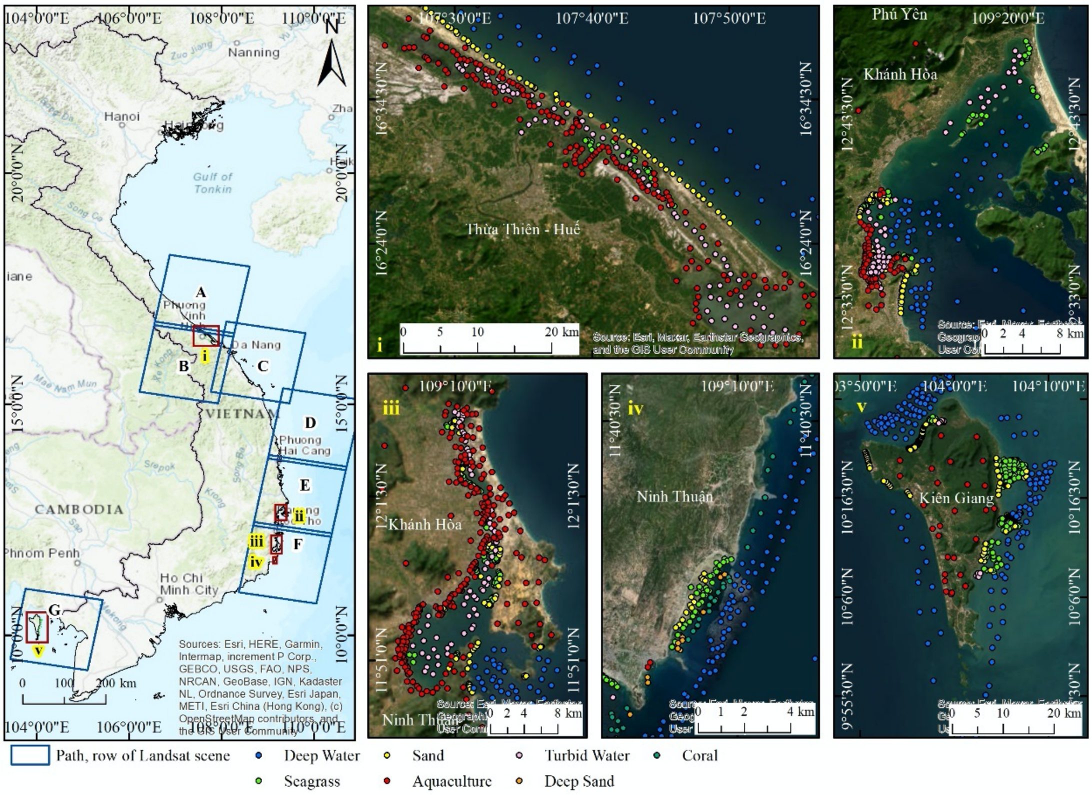

Figure 1: Landsat scenes (A-G) where seagrass could be identified from Landsat images, and specific locations (i-v) to show the training points of seven classes as ground reference data.

2.2. Data collection

2.2.1. Landsat Imagery

Seagrass mapping requires multispectral satellites with water penetrating bands, and national scale monitoring require satellites with broad spatial coverage, continuous temporal coverage (Pham et al., 2019; Hossain and Hashim, 2019). Commercial satellites are available, but for the scale of mapping required, it was impractical to purchase the data. Among satellites for which the data is publicly accessible, Landsat 4-9, Sentinel-2 and MODIS have been used for seagrass mapping. However, as Sentinel-2 constellation has only been launched in 2015, it is not suitable for decadal mapping. MODIS has coarse resolution in their VNIR bands, making it inferior to Landsat for seagrass mapping. Landsat was chosen for its overall suitability in terms of resolution, availability and accessibility.

While Landsat 4, 5, 7, 8 had data in the study period, Landsat 4 data were not chosen because the data was scarce for the study area, and Landsat 7 data were affected by scan line error. Landsat Surface Reflectance products of Landsat 5 and 8 were used for this analysis. These multispectral images are in the visible and near infrared bands (blue, green, red, near infrared, shortwave infrared). Images in those bands have 30 meters spatial resolution, and are collected at 16 days intervals. Landsat 5 started collecting images from 1984 to 2013 and Landsat 8 from 2013 until now, hence they were chosen to provide a continuous monitoring of Vietnam's coastal area. Those products have been geometrically and atmospherically corrected using the Landsat ecosystem disturbance adaptive processing system (LEDAPS) algorithm for Landsat 5 and Land Surface Reflectance Code (LaSRC) algorithms for Landsat 8 (Schmidt et al., 2013; Vermote et al., 2018). Following literature review of known seagrass sites in Vietnam, Landsat images along the coastline of Vietnam was visually inspected to identify seagrasses. However, only in the 7 Landsat scenes as indicated Figure 1 could we identify seagrass from visual interpretation. The remain areas could contain seagrass, as reported in literature survey, but were not mapped (Table S4). 496 images in 7 path-row (Table 4) were analyzed as batch processed on a cloud-based platform of Google Earth Engine. Study areas are covered by just one image. Occasionally, at the boundary of images, where there are overlaps, images were processed separately, and the mode of classification was used to present the result.

Our analysis of Landsat 5 and 8 collections revealed that the region captured by the satellite images may be offset by up to 20 km, with some outliers reaching 60 km, as seen in the "LANDSAT/LC08/C02/T1_L2/LC08_124049_20130405" and "LANDSAT/LC08/C02/T1_L2/LC08_124050_20130405" images. These discrepancies are likely the result of orbit shifts. However, the geometric correction applied to the images ensures that the features within the images are not affected by geometric errors and our analysis is not impacted by these offsets.

Images were selected to represent the dry season for each area: March to September in the northern and southern central coastal areas, and from November to April of the following year in the southern coastal area (Nguyen, 2004). Images that with more than 10% of their area masked as cloudy pixels were discarded from further processing.

2.2.2 Ground reference data

Training data were chosen via referring to previous publications, field surveys, visual interpretation, and referencing to high-resolution imagery available on Google Earth (Table 1). National surveys on seagrass distribution in Vietnam show where seagrass were referred to (Nguyen, 2008; Nguyen, 2013). Visual interpretation of Landsat images was aided with high-resolution images accessible from Google Earth Images. For visual interpretation of images where there are no high-resolution references, especially before 2000, the training data was made with the assumption that the seagrass that remain in more recent years used to exist in the same place. Training points were created for each class in each scene, spaced about 200m apart, and distributed in a grid-like manner to ensure randomness and minimize over-training. Pixels were chosen across the image to ensure good coverage of the possible variation among pixels' reflectance. Several sets of training data were created to adapt to the changing seagrass distribution. If seagrass still presents in a training data set across different time period, the same training set was used to minimize bias.

Table 1: Table of training data used for classification, presented as number of pixels

Training set	Time period	deepwater (class 0)	seagrass (class 1)	sand (class 2)	land (class 3)	turbid (class 4)	deepsand (class 5)	coral (class 6)
A1	2010-2019	48	24	53	116	35	0	0
A2	2000-2010	24	15	33	83	59	0	0
A3	1985-2000	24	64	33	24	28	0	0
B1	2010-2019	51	30	52	180	74	0	0
B2	2000-2010	34	28	53	97	148	0	0
B3	1985-2000	34	71	53	38	117	0	0
C1	2010-2019	58	11	21	99	47	0	0
C2	2000-2010	41	22	32	50	67	0	0
C3	1985-2000	41	22	35	31	67	0	0

D1	1990-2019	40	5	27	43	54	0	0
D2	1985-1990	36	15	11	29	54	0	0
E1	1990-2019	132	83	61	80	145	0	0
E2	1985-1990	86	119	50	56	83	0	0
F1	1990-2019	162	87	52	172	114	29	42
F2	1985-1990	133	154	93	172	56	36	11
G1	1990-2019	151	203	82	91	55	27	0
G2	1985-1990	50	111	27	72	103	0	0
Total		1145	1064	768	1433	1306	92	53

Two field surveys were carried out in Ninh Hai district in Ninh Thuan Province (2018) and Phu Quoc islands, Kien Giang Province (2020). In each field survey, photos of the land cover were taken along transects that were 50m apart. On the intertidal flats, trained observers walked along transects during low tides until a safe depth. Photos were taken with a GPS-enabled camera (GoPro Hero5) and iPhone 6. For surveying deeper areas, a local boat was rented to move along transects. At each point 50m apart, the GoPro camera was dropped directly below the boat, GPS location recorded on the boat, and depth measured by a depth sounder, HONDEX PS-7. Details about the land cover included: seagrass presence, seagrass species, seagrass density cover, and substrate type (sand, mud), were noted and digitized. This information was later used in creating the training data.

An unmanned aerial vehicle (UAV) was also used to take photos of seagrass beds in Phu Quoc (Figure 1-v) from 150 m altitude with 4cm resolution on 2020-02-05. Image acquisition was timed at low tide when the seagrass beds emerged from the water surface. This image was then compared with the manual interpretation of a satellite image to assess how accurate the visual interpretation is. Manual interpretation of a Landsat image, LANDSAT/LC08/C01/T1_SR/LC08_126053_20200113 without reference to the UAV image was carried out to identify seagrass and non-seagrass classes. Then a confusion matrix between my interpretation and the UAV image was done (Table S2). The overall accuracy for my interpretation was 98.69%, with Producer's accuracy for seagrass class being 99.21%, Consumer's accuracy for seagrass being 99.21%, and kappa coefficient of 0.9537. We omitted 0.79% of seagrass in this case, meaning there could be more seagrass present than my estimation. This validation of my training shows that my visual interpretation of Landsat image is adequate. However, this validation is limited as UAV images could only be orthomosaicked on shallow seafloor. Therefore, the distinction of deep seagrass from its surroundings is not validated.

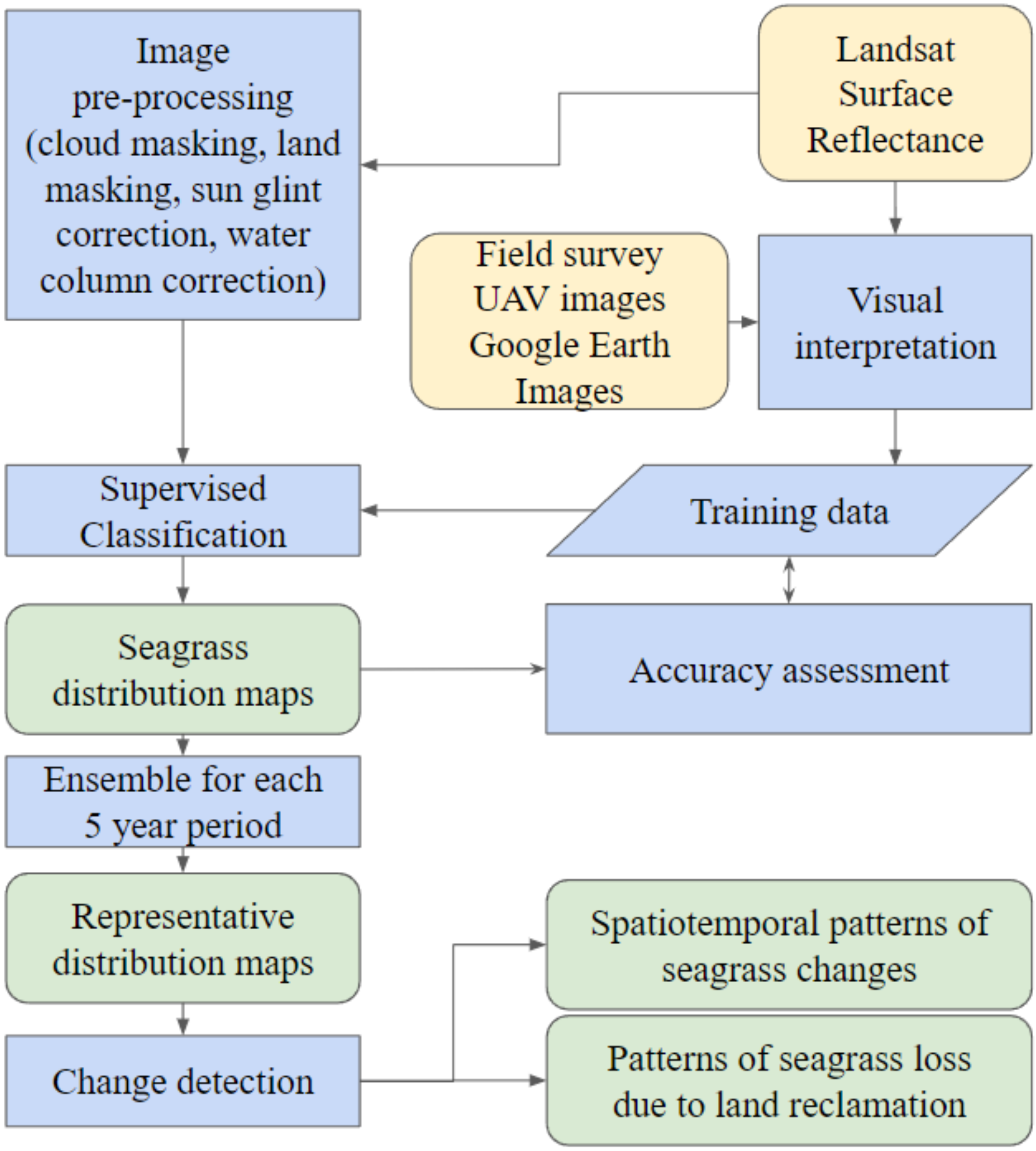

Figure 2: Flowchart of seagrass mapping.

3. Methods

Figure 2 describes the overall flow chart. While the process to map seagrass using supervised classification is well-established, it is limited to handle a nation-wide mapping. Classifying several images independently at individual sites may be result in specific, but incompatible classification results. While classifying the whole region as one image may oversimplifies the diversity in the environment as well seagrass spectral responses. Our approach aims to mitigate the problem of being overly specific or overly general by adopting a scene-wise classification. This approach allows each scene to be preprocessed with specific parameters while keeping it comparable among sites. Furthermore, the addition of the ensemble step to minimize fluctuation in estimation.

Scene-wise analysis allows for the consistent analysis of seagrass along the coastline. In addition, our approach allows for the analysis of land cover change, revealing the effects of land reclamation on seagrass beds, which have not been shown in other studies. The detail of each step is explained below.

3.1 Data preprocessing

Cloud masking was performed to eliminate cloud and cloud shadow pixels using the CFMask algorithm, represented as the QA band in the Landsat Surface Reflectance products (Foga et al., 2017). However, the LaSRC user's guide notes that "CFMask may have issues over-including bright targets such as building tops, beaches, snow/ice, sand dunes and/or salt lakes", which could potentially lead to errors in the masking of the water surface, such as wave crashes (USGS, 2020). This is unlikely to impact seagrass distribution, as seagrass tends not to be found in areas with crashing waves (Greve and Binzer, 2004).

In order to separate land from water, a land mask was created. This land mask was made by binarizing the image based on the mNDWI index (Xu, 2006). The mNDWI (modified Normalized Difference Water Index) was calculated as follows:

mNDWI = (Green - SWIR) (Green + SWIR) (1)

Where green is the reflectance of the green band (Band 2 of Landsat 5 TM, Band 3 of Landsat 8 TM) and SWIR shortwave infrared reflectance (Band 5 of Landsat 5 TM, Band 6 of Landsat 8 TM).

To monitor for changes in the coastal area over time, a baseline mask was made. Taking 1985 as the baseline, which was the earliest year Landsat 5 Surface Reflectance product was available. As for the shorelines and aquaculture ponds, the mixed pixels would have lower mNDWI than that of pure land pixels, the threshold was chosen at 0.23 to include those areas as well. The same mask was then applied to the other images.

Coastline change was observed in the coastline of Vietnam between 1990 and 2019, and especially in areas near river mouths, where accretion and erosion may both occur (Thoai, Dang, and Kim Oanh, 2019). Seagrass has been recorded to inhabit estuaries, though in our monitoring, detection of seagrass near river mouths was limited (Nguyen 2013). Another pattern of coastline change in Vietnam was due to land reclamation, as observed in this research, through classification. Using a static land mask for analysis is limited in portraying coastline changes but has benefits in showing the land-use-land-cover changes of the coastline through map-to-map comparison. If the land mask is not fixed, and is updated per image, it will be difficult to verify the occurrence of land reclamation over seagrass beds, and to calculate the area of seagrass affected by land reclamation.

Sun glint tends to contaminate the reflectance where reflectance from the water surface is captured by the satellite sensor. Images contaminated with excessive sun glint were discarded. Minor glints were corrected using Hedley's glint correction method using the NIR reflectance of the water surface (Hedley, Harborne, and Mumby 2005). Among sun glint correction methods, there are methods suitable for open ocean and shallow waters. Among sun glint correction methods for shallow waters, there are several methods available (Hochberg, Andréfouët, and Tyler 2003; Hedley, Harborne, and Mumby 2005; Lyzenga, Malinas, and Tanis 2006; Philpot 2007; Goodman, Lee, and Ustin 2008; Kutser, Vahtmäe, and Praks 2009). Among which, Philpot and Goodman's methods are calibrated for AVIRIS data, and Kutser's method requires a hyperspectral input, so they are not used here. The Hochberg, Hedley and Lyzenga methods are suitable for the dataset. Hedley's method is an improved version of Hochberg's, and Hedley's is mathematically similar with Lyzenga, while having a simpler equation, so it was chosen.

$$R'_i=R_i-b_i(R_{\mathrm{NIR}}-\mathrm{Min}_{\mathrm{NIR}}) \qquad (2)$$

Where R'i is the sun-glint corrected reflectance in band i, Ri is the reflectance in band i, bi is the regression slope of reflectance in band i against band NIR. MinNIR is the minimum value of NIR value in the sample set of pixels. The sample pixels were manually selected based on visual interpretation to create a polygon containing approximately 400 pixels (or 600m x 600m area) of deep water, including glinted pixels. Linear regressions were done to calculate bi.

To classify underwater objects, it is necessary to consider the effect of the water column. There are several methods for water column correction (Lyzenga, 1981; Sagawa et al., 2010; Matsunaga, Hoyano, and Mizukami, 2000; Stumpf, Holderied, and Sinclair, 2003). For methods that do not require auxiliary data such as bathymetry, in situ data such as attenuation coefficients, Lyzenga's Depth Invariant Index is the most well-cognized. Matsunaga's Bottom Index is mathematically identical to Lyzenga's DII, and it is more straightforward to apply. Even though Sagawa's water column correction method is effective in improving accuracy, the Bottom Reflectance Index method requires detailed bathymetry data, which is yet to be available in most coastal regions in Vietnam. Even without exact bathymetric data, Landsat images are effective for mapping seagrass in tropical coastal waters. Matsunaga's Bottom Index, which is derived from Lyzenga's Depth Invariant Index, proposed a simpler representation:

$$BI_{ij}=\ln(L_i-L_{si})-k_{ij}*\ln(L_j-L_{sj}) \qquad (3)$$

Where kij is the extinction ratio of bands i to j. It is given by calculating the gradient from the regression analysis between signals of two bands i, j over an area of identical substrate with varying depth. Three Bottom Indices were calculated using 3 pairs of Blue-Green, Blue-Red, and Green-Red bands.

To calculate the attenuation coefficients, for a site, one area with a homogeneously sandy substrate with varying depth was chosen by visual interpretation. Then a polygon was drawn to sample about 50 pixels along that transect. Assuming the water quality is horizontally homogeneous, the location of the transect should not significantly affect the calculated coefficients if it samples enough pixels to establish pair-wise linear correlations. Linear regression was done on the sampled pixel values to calculate the attenuation coefficients for 3 pairs of bands: Blue-Green, Blue-Red, and Green-Red. Then, the attenuation coefficient was used to calculate the Bottom Indices, which are supposed to represent the bottom reflectance if the water column effect were corrected.

3.2 Supervised Classification

Supervised classification was used to monitor the areal changes of seagrass and other classes. Classes were chosen to have distinct spectral responses. A comprehensive class scheme was created for the entire country, containing 7 classes, described below:

The class of interest is seagrass, with low reflectance in most bands, and higher reflectance in the green band. In previous, it has been shown that there were few differences detectable with the specifications of Landsat 5 and 8 for the classes of seagrass and seaweed, hence the class of seagrass might include seaweed. (Kakuta, Takeuchi, and Prathep 2016). Nevertheless, as confirmed with literature review and our field surveys, the areas of training for seagrass contain dominantly seagrass, with minimal inclusion of seaweed.

Non-seagrass classes include:

- Deep water, usually at the deep side of the coast, typically more than 5m deep in tropical coast, universally low reflectance, except for blue bands.
- Sand, usually on the shallow side of the coast, may include sandy substrates mixed with dead corals, and mud; with higher reflectance in the red, green, and blue band, but low in NIR.
- Land features are emerged features are pixels representing objects above the sea surface, notably reclaimed land, aquaculture ponds, boats, or other man-made structures, which usually have high NIR reflectance.
- Turbid water denotes pixels where the water column's reflectance totally obscures the reflectance of the bottom cover, usually in

estuarine and lagoon systems. Though it is possible that seagrass may still exists under the turbid water column, it is inconclusive, hence needs to be verified through field surveys.

- Deep sand denotes sandy substrate under a clear water column.
- Coral denotes coral reefs.

Figure 3 shows the spectral response signatures of different classes involved in seagrass mapping. Deep water pixels have overall low reflectance. The spectral responses of seagrass and turbid water are similar in the optical bands. This could be a source of confusion for further classification in seagrass mapping in tropical coastal waters.

To verify the separability among the classes, the Jeffries-Matusita Distance (JM distance) was calculated (Table 2). The JM distance is a commonly used criterion in the field of pattern recognition and feature selection. The JM distance (J) between two classes w_i and w_j that are members of a set of C classes (i, j = 1, 2, …, C, i ≠ j) has been defined as follows (Davis et al., 1978):

$$J_{ij} = 2(1 - e^{-d_{ij}}) \qquad (4)$$

where d_{ij} is the Bhattacharyya distance between the classes w_i and w_j, defined as (Davis et al., 1978):

$$d_{ij} = \left\{ \int \sqrt{P(\frac{x}{w_i})P(\frac{x}{w_j})}dx \right\} \quad (5)$$

where $P(x/w_i)$ and $P(x/w_j)$ are the conditional probability density functions of the random variable x, given the data classes w_i and w_j, respectively.

Table 2: Jeffries-Matusita Distance of training points sampled on the test image

	Deep water	**Seagrass**	**Sand**	**Land**	**Turbid**	**Deep sand**	**Coral**
Deep water	-						
Seagrass	1.411	-					
Sand	1.414	1.358	-				
Land	1.414	1.387	1.359	-			
Turbid	1.400	1.359	1.388	1.412	-		
Deep sand	1.410	1.407	1.406	1.414	1.375	-	
Coral	1.352	1.413	1.414	1.414	1.410	1.412	-

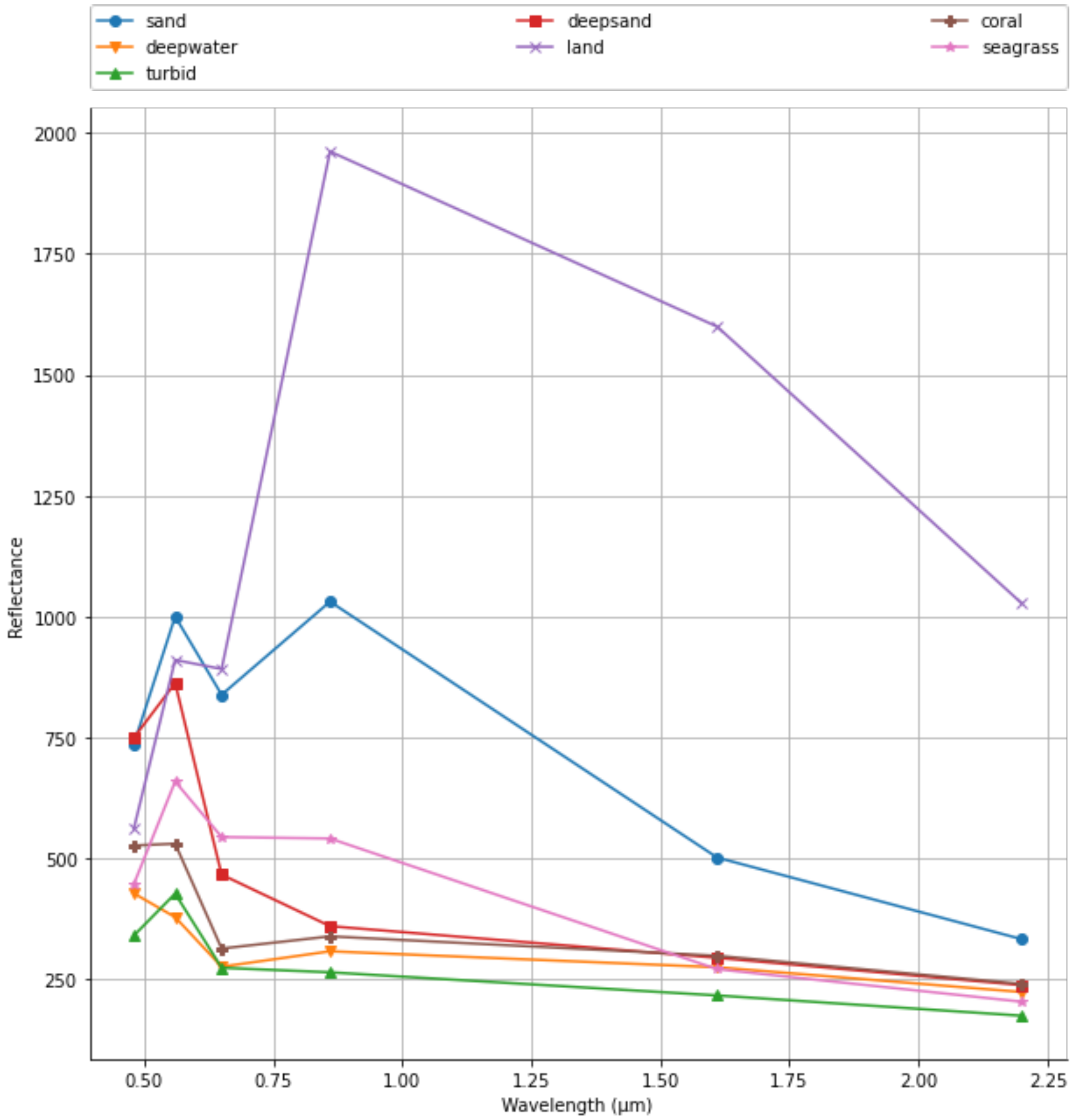

Figure 3: Spectral responses of points in seven classes sampled on LANDSAT/LC08/C01/T1_SR/LC08_123052_20160909 image.

JM distance shows the separability between classes, with values ranging from 0 to 2, where 0 means the two distributions are identical, and 2 means they are totally different. All of the 7 classes in this test image had a JM distance of between 1.352 to 1.414, showing that they are sufficiently separable. Seagrass is less separable from Sand and Turbid class than from other classes, which might show as errors in the classification step.

In this study, a Random Forest classifier with 100 trees was utilized for the classification task. The Random Forest algorithm is an ensemble method that involves the construction of multiple decision trees, with the final classification result determined by the mode of the classifications provided by each individual tree (Breiman, 2001; Ho, 1995).

This method was chosen for its high accuracy in land cover classification, as well as its relatively low computational demands compared to other machine learning algorithms such as Support Vector Machine, or deep learning algorithms, while having adequate classification accuracy (Komatsu et al., 2020). The parameter of 100 trees was selected as a balance between the desire for high accuracy and the constraint of limited computational resources, following a process of trial and error. Inputs for the classifiers include the blue, green, red, near infrared, shortwave infrared 1, shortwave infrared 2, Bottom Index Blue-Green, Bottom Index Blue-Red, Bottom Index Green – Red. To adjust for variations among images, especially in the water column, the classifier was trained for every image. Using the training data set as described in Table 1, the image would be sampled to train a random forest classifier for the specific image, which was in turn used to classify the image.

Ensembling was done to minimize salt and pepper error, and enhance consistency among regions. Classification of seagrass in tropical coastal waters is challenging because the classifier has difficulty detecting seagrass in turbid waters. In tropical coastal waters, high turbidity and constantly changing water quality mean the reflectance of seagrass pixels could be obscured by the water column. As a result, a seagrass pixel may be classified as seagrass in one image, and as turbid water in another image in the same location. To get the most representative land cover class, the statistical mode of classification results in each 5 years period was used as the representative class for that pixel (Figure S1). We made sure that there are at least 3 images per five-year stack for the statistical analysis. The area of seagrass was calculated based on the ensembled results. The number of pixels was multiplied by one pixel's area to give the total area of a class in the image.

For each image, we split the training data into 70% for training and 30% for validation. We trained a classifier on the 70% training data and then compared the resulting classification with the validation data. We repeated this process 100 times and used the mean accuracy across the 100 repetitions to evaluate the accuracy of the classifier for each image. We then took the mean of all the individual image accuracies to arrive at "mean overall accuracy", "mean producer accuracy for seagrass" and "mean user accuracy for seagrass" for the entire time series of images. The study assumed that the accuracy of the time series product is equivalent to the accuracy of the thematic mapping (Lyons, Roelfsema, and Phinn, 2013).

Change detection was done to identify what may have caused the changes in seagrass distribution. Classified maps before and after were compared to create a transition map. The pixel value on the transition map shows the class of that pixel in the map before and after, summarized

Table S5. Changes were summarized as: seagrass remained, seagrass lost to land features, seagrass lost to turbid water, seagrass lost to other classes, and seagrass gained. Other changes were not analyzed. Seagrass lost to land features would suggest that seagrass was lost due to land reclamation, while seagrass lost to turbid water may suggest a worsened water quality

4. Results and Discussions

4.1 Classification results

Table 3 shows the confusion matrix for the test image. The results of the classification analysis yielded an overall accuracy of 84.62% and a kappa coefficient of 0.81, indicating a satisfactory level of agreement between the classification results and the reference data. The producer's accuracy for seagrass was found to be 90.00%, indicating that 10% of seagrass was incorrectly classified as sand. Conversely, the consumer's accuracy was 75%, indicating that sand, land features, and turbid water were misclassified as seagrass. This may be attributed to the similarities in appearance between seagrass and these other classes, as illustrated in Table 2.

Table 4 shows the number of images used and the accuracy assessment of the classification results for images in the paper. The number of available images differs due to the frequency of cloud contamination. The mean overall accuracy ranges from 75.8% to 90.4%; the mean producer accuracy for the seagrass class ranges from 40.8% to 77.9%; the mean user accuracy for the seagrass class ranges from 37.1% to 73.4%.

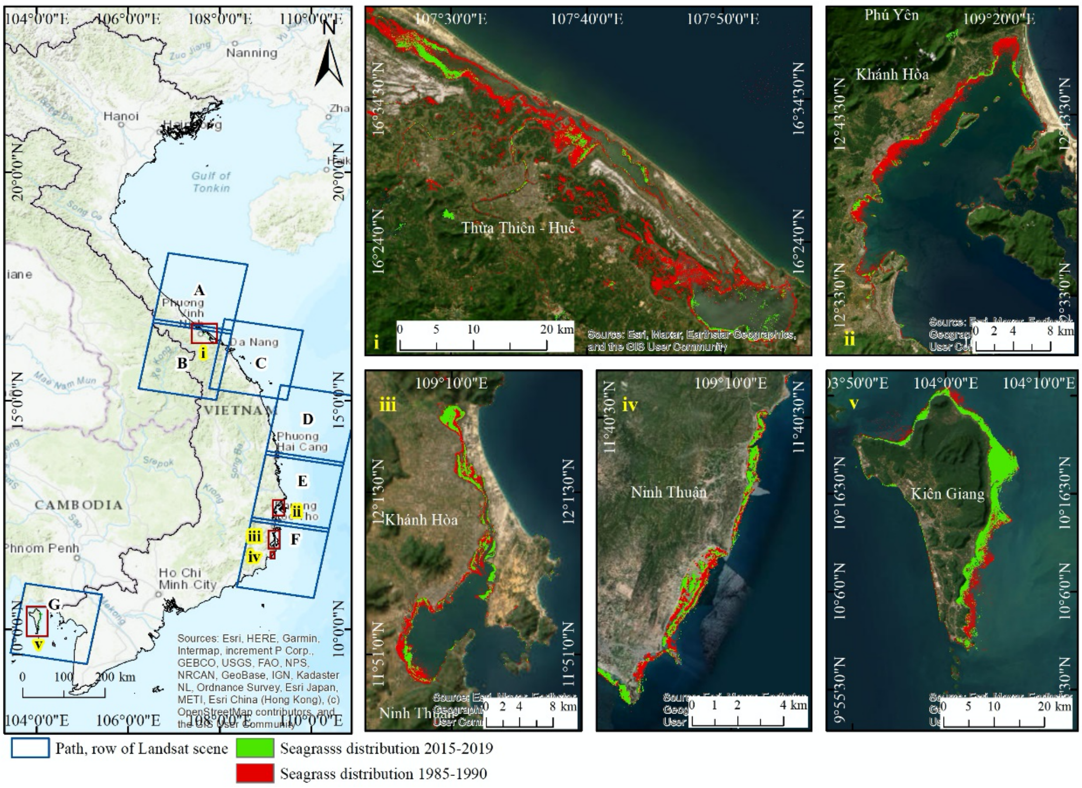

Figure 4. Changes in seagrass extent in Vietnam's major seagrass beds at (i) Tam Giang Lagoon, (ii) Van Phong Bay, (iii) Thuy Trieu Lagoon and Cam Ranh Bay, (iv) Thai An and My Hoa, and (v) Phu Quoc island. Seagrass extent analyzed in 1985-1990 and 2015-2019 periods were shown to observe their changes.

Table 3. Confusion matrix for the test image (LANDSAT/LC08/C01/T1_SR/LC08_123052_20160909)

		Classified								
		Deep water	**Seagrass**	**Shallow sand**	**Land features**	**Turbid water**	**Deep sand**	**Coral**	**Total**	**Producer's Accuracy**
Reference	**Deep water**	39	0	0	0	0	0	0	39	100.00%
	Seagrass	0	18	2	0	0	0	0	20	90.00%
	Shallow sand	0	2	9	3	2	2	0	18	50.00%
	Land features	0	2	2	27	0	0	0	31	87.10%
	Turbid water	0	2	0	0	27	3	1	33	81.82%
	Deep sand	0	0	0	0	1	7	1	9	77.78%
	Coral	0	0	0	0	1	0	5	6	83.33%
	Total	39	24	13	30	31	12	7	156	
	Consumer's accuracy	100.0%	75.0%	69.2%	90.0%	87.1%	58.3%	71.4%		

Table 4. Accuracy assessment of classification

Landsat scene	Number of images classified	Mean overall accuracy	Mean producer's accuracy for seagrass	Mean consumer's accuracy for seagrass
A	27	82.8%	58.8%	69.3%
B	69	84.3%	40.8%	37.1%
C	66	75.8%	49.4%	58.7%
D	168	90.4%	43.1%	47.7%
E	65	76.4%	64.9%	72.4%
F	55	77.8%	67.6%	63.4%
G	46	83.5%	77.9%	73.4%

This research presents a comprehensive analysis of the temporal and spatial patterns of seagrass distribution changes in Vietnam over a 30-year period (1985-2019) using a cloud-based monitoring framework. Figure 4 illustrates the major seagrass sites that were monitored, while Table S3 provides a detailed breakdown of the area of seagrass sites during two distinct time periods (1985-1990 and 2015-2019) and their comparison. The total area of seagrass beds in Vietnam during the 1985-1990 period was 36 ha, while during the 2015-2019 period, it was 17,081 ha. The study indicates that seagrass beds larger than 50 ha in lagoons, bays, and tidal flats were effectively monitored. However, it must be noted that not all seagrass sites in Vietnam could be mapped, particularly those located in northern Vietnam.

This study presents a national-scale framework for monitoring seagrass beds in Vietnam over a 30-year period utilizing remote sensing imagery. The proposed method allows for consistent monitoring of most seagrass beds in Vietnam, even those smaller than 100 ha. However, it should be noted that the framework may have missed 1654-4018 ha of seagrass. Through visual inspection of Landsat images for the entire coastline of Vietnam, seagrass beds were not identified in certain areas listed in Table S4. This may be due to a combination of factors such as small seagrass area extent, low seagrass density, difficulty in observing specific seagrass species, and poor water quality. It is important to note that in this analysis, all seagrass pixels in one image were assumed to be of the same class, which may be an oversimplification. The spectral response of seagrass can vary depending on several physical factors, such as the seagrass species present, the water column, and the substrate. These factors can influence the seagrass spectral response, making it difficult to accurately classify all seagrass pixels as the same class. For example, dense seagrass patches of *Enhalus acoroides*, *Thalassia hemprichii*, *Cymodocea rotundata*, and *Cymodocea serrulate* could be recognized, but smaller species such as *Halophila ovalis, Halodule uninervis* were more difficult to distinguish.

The classification accuracy obtained in this study is consistent with previous research that utilizes pixel-based classifications, as reported in the literature (Lyons, Phinn, and Roelfsema, 2012; Chen et al., 2016; Hossain et al., 2019). However, the accuracy varied across different scenes (path, row) of Landsat images, as shown in Table 4. This variation could be attributed to variations in the dominant habitat type and seagrass species in the respective scenes.

The results of the classification are presented in Figure S 1, where seagrass is depicted in green and non-seagrass classes are illustrated in black. The ensemble result is also included. It is observed that there are variations in the distribution of seagrass in individual images, which may be attributed to factors such as changes in water quality, image quality, or classification errors. As these images were acquired during the same season, it is unlikely that there would be significant changes in the distribution of seagrass beds. To mitigate this fluctuation, the mode of classification was utilized to present a representative distribution of seagrass over a five-year period. The current method also emphasizes the detection of permanent changes in land cover, such as land reclamation on seagrass beds.

Water column correction was applied scene-wise, which may have some caveats. These assumptions were made while applying the bottom index technique for water column correction. Firstly, it was assumed that the water quality is horizontally identical in the whole Landsat image. This may not be true in coastal areas where there are significant sources of mixing or loading such as river mouths or areas with heavy aquaculture activities, or in places with highly varied coastal environments such as in Figure 1-iv, with a lagoon, bay, and exposed waters in the same image. Secondly, it was assumed that the bottom reflectance was not completely absorbed by the water column, or objects on the water surface, which may not be true in turbid areas. Thirdly, the water column is between two and ten meters deep. In very shallow water (less than two meters deep), Lyzenga's equation does not correct the effect of internal reflections, especially where light is continuously reflected between the water surface and a bright bottom surface, such as sand. For waters deeper than 10m, red and green light has mostly attenuated, leaving no reflectance to refer to for calculation. Because of those assumptions, the bottom indices are not totally reliable for the accurate classification of benthic types in the coastal waters of Vietnam, which is typically turbid.

4.2 Spatial and temporal patterns of seagrass in Vietnam in 1985-2019

Table-S3 shows the area of seagrass beds in Vietnam and their changes in the 30 years period. Most of the seagrass beds have declined, with a few exceptions of increased or maintained relatively stable. The rate of decline was further explored in Figure 5, which shows that across three types of habitats, seagrass beds all over the coastline of Vietnam have been decreasing. Relative changes were presented in different habitats of the seagrass beds, as each of them has distinctive characteristics.

The most severely damaged seagrass beds are seagrass beds in bays and lagoons, where 60% to 85% of seagrass beds were lost between 1985 and 2019. Seagrass beds on tidal flats have also decreased, but to a lesser extent, ranging from a 67% loss in Vinh Hao to a 15% gain in Bai Bon. Overall, 53% of seagrass areas monitored in this analysis were lost, down from 36,185 ha in the 1985-1990 period to 17081 ha in the 2015-2019 period. 8 sites had a more than 70% loss of seagrass. In the temporal pattern aspect, most seagrass beds decrease before 2000. From 2005-2019, the decrease continued, with various patterns depending on sites.

There are many factors contributing to the loss of seagrass beds, from anthropogenic factors such as destructive fishing, land reclamation for construction, building aquaculture ponds, water pollution, and natural factors such as typhoons but this analysis focuses on the loss of seagrass beds due to land reclamation because this irreversible change is the most serious(Nguyen, 2004; Nguyen, 2013). Figure 6 shows that in bays and lagoons systems, land reclamation happens extensively in almost all seagrass beds, as well as a few tidal flats.

Figure 7 highlights the significant loss of seagrass due to land reclamation in Cam Ranh Bay. The shallow areas inside the bay have been extensively developed for aquaculture ponds and infrastructures such as piers and ports. The other changes, such as seagrass pixels turning into turbid water pixels, are also worth considering. However, interpreting those changes requires further data, such as measuring water quality, to be conclusive.

Seagrass losses in Vietnam are attributed to destructive fishing methods, agricultural reclamation, aquaculture, tourism, marine transportation and construction of ports, typhoons, and degrading water quality (Nguyen, 2008). Similarly, in national seagrass report, a compiled study of 37 seagrass beds comparing their areas in 1997-2000 and 2009-2010 showed 20 out of 37 seagrass beds were damaged by reclamation for construction or aquaculture, 3 due to flood-caused sediment burials, 2 due to destructive fishing, 12 with unclear causes (Nguyen, 2013).

Our study quantified the observation that reclamation is a major cause of seagrass loss in Vietnam and gave insights into the spatial and temporal patterns of reclamation-driven loss of most seagrass beds along the Vietnamese coastline. This observation agrees with (Chen et al. 2016), (Vo et al. 2020), and our study further quantified the area of loss due to land reclamation, as well as extending the area of monitoring to the whole Vietnam coastline. This result provided the foundation for further discussion of seagrass loss and its causes in Vietnam.

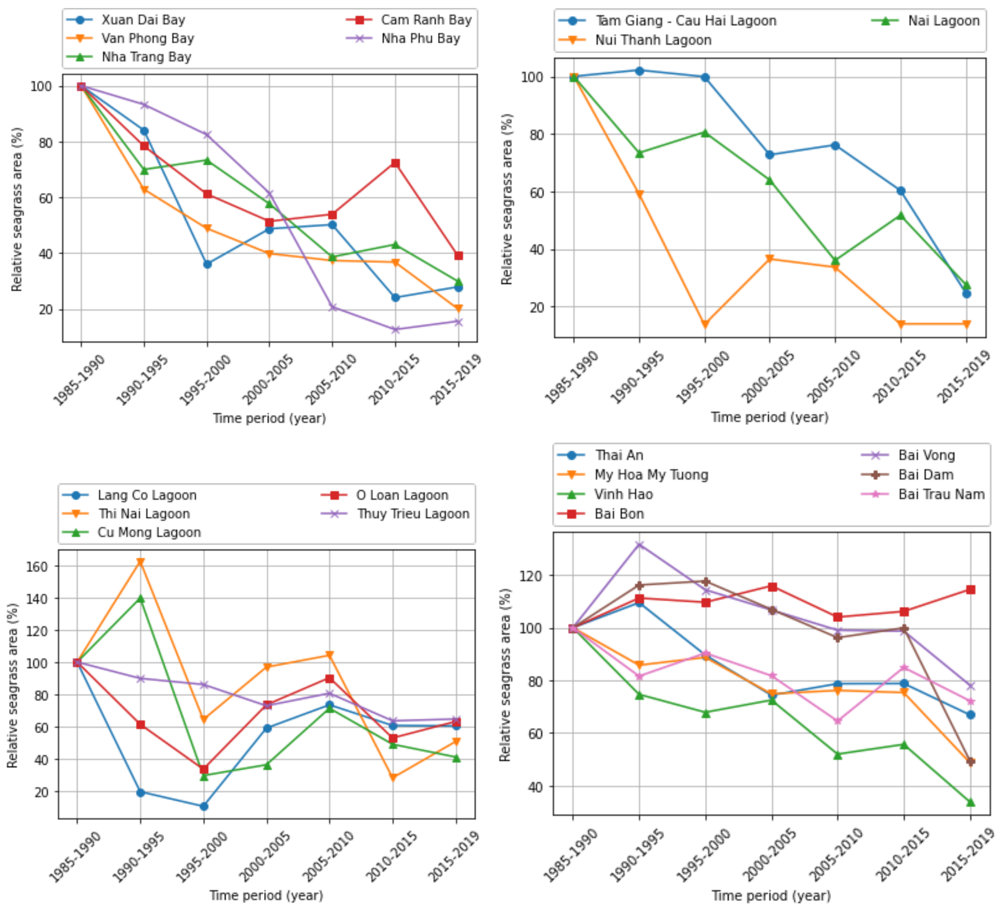

Figure 5: Relative seagrass area changes of seagrass beds in Vietnam's coastal zone

from 1985 to 2019.

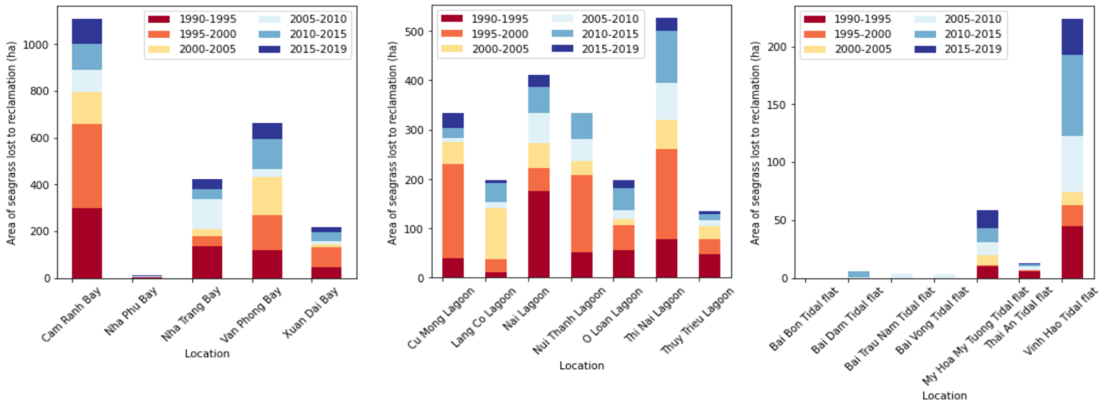

Figure 6: Area of seagrass beds being replaced by land features such as aquaculture ponds or piers in respective ecosystems: (a) Major bays, (b) Major lagoons, (c) Major tidal flats between each 5 years periods.

The temporal trend of seagrass loss to land reclamation seems to suggest that most losses happened in the 1990s up until 2005 (Figure 6). Such a trend is explained partially by land use policies. National Decree 773-TTg approved on December 21, 1994, strongly encouraged people to clear coastal wetlands and reclaim coastal waterfronts for shrimp farming (Le, 2008). These movements could have had a similar impact on coastal seagrass beds, which received even less attention from conservation back then. Conversion of seagrass beds to land features has slowed down from 2005 onwards, perhaps due to improvements in coastal ecosystem conservation policies. However, it could also be explained that the shallow coastal land that is easy to be reclaimed has already been reclaimed, leaving only the deeper, more expensive to convert areas.

In our study, degraded water quality, shown as seagrass lost to turbid water (Figure 7) is also suggested to be a major contributor to seagrass loss, which is also suggested by other studies (Quang et al., 2017). Sea level rise leading to coastline receding inland is a possible phenomenon. The methodology of this paper, unfortunately, cannot be quantitatively conclusive about coastal erosion. As we fixed a baseline coastline, and analyze how the coastal seagrass has changed, coastal erosion resulting in the coastline receding will be unknown. The status of such eroded land could be formations of sand banks or tidal flats, or even potentially seagrass (Veettil et al., 2021; Thuc et al., 2023; T. T. H. Pham and Furukawa, 2007). As a result, it may result in a landward expansion of seagrass distribution. As we could not identify such changes in our analysis, we assume an underestimation in this aspect. Besides, sea level rise may result in a deeper water column over established seagrass meadows, leading to the loss of seagrass in the deep edge. The detection of seagrass loss in the deep edge, however, is also limited in this paper, as it is inconclusive whether seagrass was truly lost in the deeper area or is not detected through the satellite image.

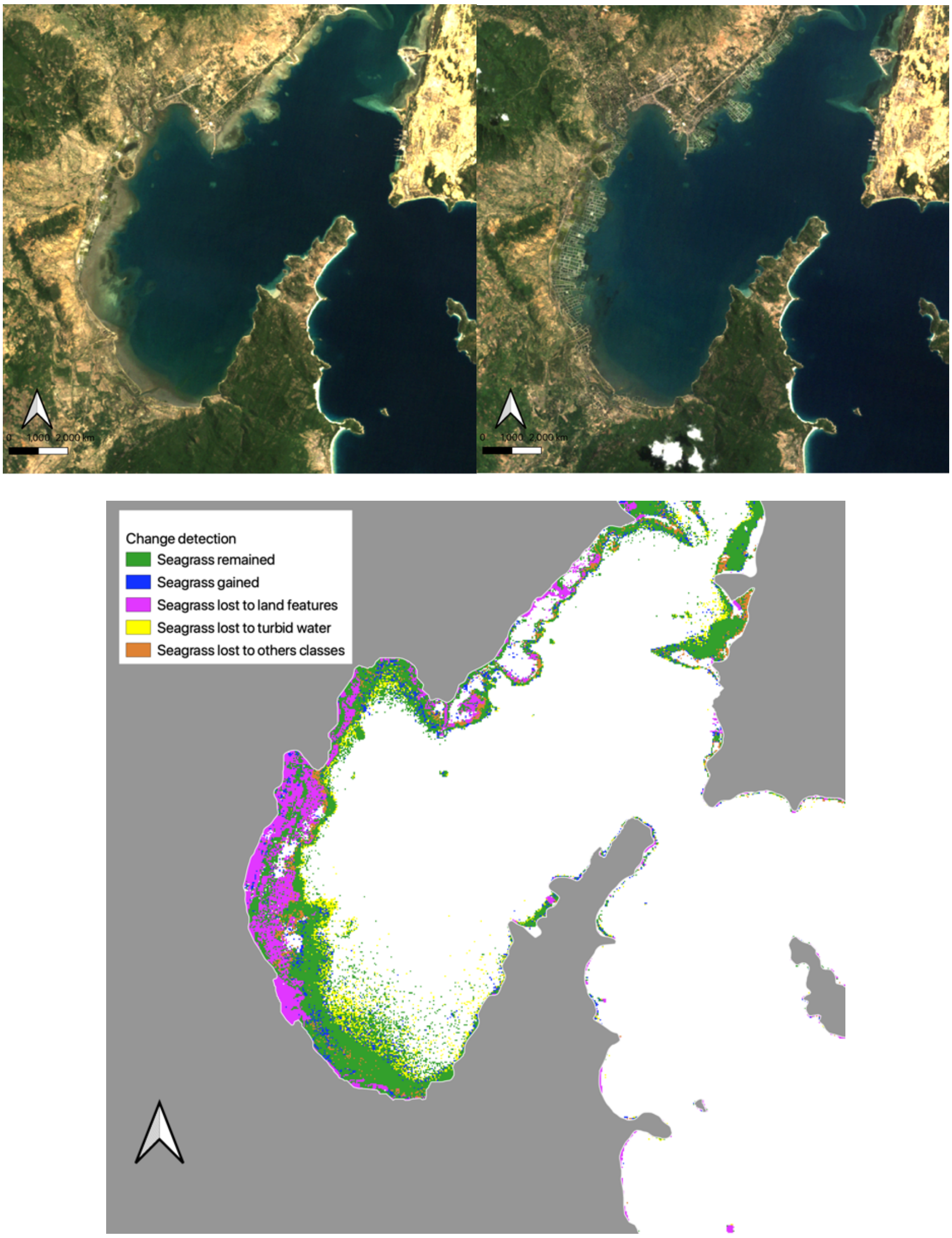

Figure 7. Change detection at Cam Ranh Bay (Figure 1-iv). True color images of 1990-07-16 (top left) and 1996-06-30 (top right) show the replacement of seagrass beds by land reclamation for aquaculture ponds and Map-to-map change detection between the 1990-1995 period and 1995-2000 period.

5. Conclusion

We were able to monitor the changes in most seagrass beds in Vietnam for more than 30 years, showing explicitly the temporal and spatial patterns of seagrass area changes. We could map 36,185 ha of seagrass in 1985-1990 period and 17,081 ha in 2015-2019 period, showing a 52.79% of seagrass loss. Most seagrass beds were lost between the late 1990s and early 2000s and continued to decrease. The continued decrease signified the lack of effective conservation and recovery for seagrass ecosystems. Spatial patterns showed that most seagrass losses were directly displaced by land reclamation for aquaculture or construction of infrastructure. These findings demonstrated that remote sensing is a cost-effective method to monitor coastal seagrass ecosystems at this spatial and temporal scale. The results emphasized the necessity and urgency to update the seagrass distribution data, as many seagrass beds have decreased in size or disappeared totally. It is potential to apply this approach to monitor other regions to enhance our understanding of changes to seagrass ecosystems and improve our conservation.

References

[1] Breiman, Leo. 2001. “Random Forests.” Machine Learning 45: 5–32. doi:10.1201/9780367816377-11.

[2] Cao, Van Luong, Duc Tien Dam, and Cong thung Do. 2005. “Seagrass of the Western Coastal Zone of the Gulf of Tonkin, Vietnam,” no. July 2016. doi:10.15625/1859-3097/14/3A/5196.

[3] Cao, Van Luong, Duc Tien Dam, and Thi Phương Anh Tran. 2019. “Results on Assessment of Organic Carbon Storage Capacity of Seagrass Beds in Some Typical Coastal Lagoons.” doi:10.15625/vap.2019.000183.

[4] Cao, Van Luong, Van Thao Nguyen, Teruhisa Komatsu, Dac Ve Nguyen, and Duc Tien Dam. 2012. “Status and Threats on Seagrass Beds Using GIS in Vietnam.” Remote Sensing of the Marine Environment II 8525 (October): 852512. doi:10.1117/12.977277.

[5] Chen, Chi Farn, Va Khin Lau, Ni Bin Chang, Nguyen Thanh Son, Phuoc Hoang Son Tong, and Shou Hao Chiang. 2016. “Multi-Temporal Change Detection of Seagrass Beds Using Integrated Landsat TM/ETM +/OLI Imageries in Cam Ranh Bay, Vietnam.” Ecological Informatics 35 (January). Elsevier B.V.: 43–54. doi:10.1016/j.ecoinf.2016.07.005.

[6] Davis, S. M., D. A. Landgrebe, T. L. Phillips, P. H. Swain, R. M. Hoffer, J. C. Lindenlaub, and L. F. Silva. 1978. “Remote Sensing: The Quantitative Approach.” Mhi. https://ui.adsabs.harvard.edu/abs/1978mhi..book.....D/abstract.

[7] Duarte, Carlos M., Núria Marbà, Esperança Gacia, James W. Fourqurean, Jeff Beggins, Cristina Barrón, and Eugenia T. Apostolaki. 2010. “Seagrass Community

Metabolism: Assessing the Carbon Sink Capacity of Seagrass Meadows." Global Biogeochemical Cycles 24 (4): 1–8. doi:10.1029/2010GB003793.
[8] Foga, Steve, Pat L. Scaramuzza, Song Guo, Zhe Zhu, Ronald D. Dilley, Tim Beckmann, Gail L. Schmidt, John L. Dwyer, M. Joseph Hughes, and Brady Laue. 2017. "Cloud Detection Algorithm Comparison and Validation for Operational Landsat Data Products." Remote Sensing of Environment 194. Elsevier Inc.: 379–390. doi:10.1016/j.rse.2017.03.026.
[9] Fourqurean, James W., Carlos M. Duarte, Hilary Kennedy, Núria Marbà, Marianne Holmer, Miguel Angel Mateo, Eugenia T. Apostolaki, et al. 2012. "Seagrass Ecosystems as a Globally Significant Carbon Stock." Nature Geoscience 5 (7). Nature Publishing Group: 505–509. doi:10.1038/ngeo1477.
[10] Goodman, James A., Zhong Ping Lee, and Susan L. Ustin. 2008. "Influence of Atmospheric and Sea-Surface Corrections on Retrieval of Bottom Depth and Reflectance Using a Semi-Analytical Model: A Case Study in Kaneohe Bay, Hawaii." Applied Optics, Vol. 47, Issue 28, Pp. F1-F11 47 (28). Optica Publishing Group: F1–F11. doi:10.1364/AO.47.0000F1.
[11] Greve, Tina M., and T. Binzer. 2004. "Which Factors Regulate Seagrass Growth and Distribution?" European Seagrasses: An Introduction to Monitoring and Management, 19–23.
[12] Hedley, J. D., A. R. Harborne, and P. J. Mumby. 2005. "Simple and Robust Removal of Sun Glint for Mapping Shallow-Water Benthos." International Journal of Remote Sensing 26 (10): 2107–2112. doi:10.1080/01431160500034086.
[13] Hedley, John D., Brandon J. Russell, Kaylan Randolph, Miguel Pérez-Castro, Román M. Vásquez-Elizondo, Susana Enríquez, and Heidi M. Dierssen. 2017. "Remote Sensing of Seagrass Leaf Area Index and Species: The Capability of a Model Inversion Method Assessed by Sensitivity Analysis and Hyperspectral Data of Florida Bay." Frontiers in Marine Science 4 (NOV): 1–20. doi:10.3389/fmars.2017.00362.
[14] Ho, Tin Kam. 1995. "Random Decision Forests." Proceedings of the International Conference on Document Analysis and Recognition, ICDAR 1. IEEE Computer Society: 278–282. doi:10.1109/ICDAR.1995.598994.
[15] Hoang Cong Tin, Luong Quang Doc, and Ho Thi Thuy Uyen. 2020. "Quantifying Shoot Density and Biomass of Seagrass Beds in the Central Coast of Vietnam." Journal of Environmental Science and Engineering B 9 (2): 56–70. doi:10.17265/2162-5263/2020.02.002.
[16] Hochberg, Eric J., Serge Andréfouët, and Misty R. Tyler. 2003.

"Sea Surface Correction of High Spatial Resolution Ikonos Images to Improve Bottom Mapping in Near-Shore Environments." IEEE Transactions on Geoscience and Remote Sensing 41 (7 PART II): 1724–1729. doi:10.1109/TGRS.2003.815408.

[17] Hossain, Mohammad Shawkat, Japar Sidik Bujang, Muta Harah Zakaria, and Mazlan Hashim. 2015. "The Application of Remote Sensing to Seagrass Ecosystems: An Overview and Future Research Prospects." International Journal of Remote Sensing 36 (1). Taylor & Francis: 61–114. doi:10.1080/01431161.2014.990649.

[18] Hossain, Mohammad Shawkat, and Mazlan Hashim. 2019. "Potential of Earth Observation (EO) Technologies for Seagrass Ecosystem Service Assessments." International Journal of Applied Earth Observation and Geoinformation 77 (October 2018). Elsevier: 15–29. doi:10.1016/j.jag.2018.12.009.

[19] Hossain, Mohammad Shawkat, Mazlan Hashim, Japar Sidik Bujang, Muta Harah Zakaria, and Aidy Mohammad Muslim. 2019. "Assessment of the Impact of Coastal Reclamation Activities on Seagrass Meadows in Sungai Pulai Estuary, Malaysia, Using Landsat Data (1994–2017)." International Journal of Remote Sensing 40 (9). Taylor & Francis: 3571–3605. doi:10.1080/01431161.2018.1547931.

[20] Kakuta, Satomi, Wataru Takeuchi, and Anchana Prathep. 2016. "Seaweed and Seagrass Mapping in Thailand Measured Using Landsat 8 Optical and Textural Image Properties." Journal of Marine Science and Technology (Taiwan) 24 (6): 1155–1160. doi:10.6119/JMST-016-1026-4.

[21] KOMATSU, Teruhisa, Mazlan HASHIM, Nurjannah NURDIN, Thidarat NOIRAKSAR, Anchana PRATHEP, Milica STANKOVIC, Tong SON, et al. 2020. "Practical Mapping Methods of Seagrass Beds by Satellite Remote Sensing and Ground Truthing." Coastal Marine Science 43 (1): 1−25.

[22] Kutser, Tiit, Ele Vahtmäe, and Jaan Praks. 2009. "A Sun Glint Correction Method for Hyperspectral Imagery Containing Areas with Non-Negligible Water Leaving NIR Signal." Remote Sensing of Environment 113 (10). Elsevier: 2267–2274. doi:10.1016/J.RSE.2009.06.016.

[23] Lau, Va-khin, Chi-farn Chen, and Hoang-Son Tong Phuoc. 2013. "Mapping Seagrass Beds and Coral Reefs in the Coastal of Ninh Hai District , Ninh Thuan Province of Vietnam Using Landsat 8 Oli Image" 2013 (May): 1–6.

[24] Le, Hue. 2008. "Economic Reforms and Mangrove Forests in Central Vietnam." Society & Natural Resources 21 (2): 106–119. doi:10.1080/08941920701617775.

[25] Lyons, Mitchell B., Stuart R. Phinn, and Chris M. Roelfsema. 2010. "Long Term Monitoring of Seagrass Distribution in Moreton Bay, Australia, from 1972-2010 Using Landsat MSS, TM, ETM+." International Geoscience and Remote Sensing Symposium (IGARSS), 5–8. doi:10.1109/IGARSS.2010.5651878.

[26] Lyons, Mitchell B., Stuart R. Phinn, and Chris M. Roelfsema. 2011. "Long Term Land Cover and Seagrass Mapping Using Landsat Sensors from 1972 - 2010 in the Coastal Environment of South East Queensland, Australia." In 34th International Symposium on Remote Sensing of Environment - The GEOSS Era: Towards Operational Environmental Monitoring.

[27] Lyons, Mitchell B., Stuart R. Phinn, and Chris M. Roelfsema. 2012. "Long Term Land Cover and Seagrass Mapping Using Landsat and Object-Based Image Analysis from 1972 to 2010 in the Coastal Environment of South East Queensland, Australia." ISPRS Journal of Photogrammetry and Remote Sensing. doi:10.1016/j.isprsjprs.2012.05.002.

[28] Lyons, Mitchell B., Chris M. Roelfsema, and Stuart R. Phinn. 2013. "Towards Understanding Temporal and Spatial Dynamics of Seagrass Landscapes Using Time-Series Remote Sensing." Estuarine, Coastal and Shelf Science 120. Elsevier Ltd: 42–53. doi:10.1016/j.ecss.2013.01.015.

[29] Lyzenga, David R. 1978. "Passive Remote Sensing Techniques for Mapping Water Depth and Bottom Features." Applied Optics 17 (3): 379. doi:10.1364/ao.17.000379.

[30] Lyzenga, David R. 1981. "Remote Sensing of Bottom Reflectance and Water Attenuation Parameters in Shallow Water Using Aircraft and Landsat Data." International Journal of Remote Sensing 2 (1): 71–82. doi:10.1080/01431168108948342.

[31] Lyzenga, David R., Norman P. Malinas, and Fred J. Tanis. 2006. "Multispectral Bathymetry Using a Simple Physically Based Algorithm." IEEE Transactions on Geoscience and Remote Sensing 44 (8): 2251–2259. doi:10.1109/TGRS.2006.872909.

[32] Matsunaga, Tsuneo, Akira Hoyano, and Yosei Mizukami. 2000. "Monitoring of Coral Reefs on Ishigaki Island in Japan Using Multitemporal Remote Sensing Data." Hyperspectral Remote Sensing of the Ocean 4154: 212–222. doi:10.1117/12.411677.

[33] McLeod, Elizabeth, Gail L. Chmura, Steven Bouillon, Rodney Salm, Mats Björk, Carlos M. Duarte, Catherine E. Lovelock, William H. Schlesinger, and Brian R. Silliman. 2011. "A Blueprint for Blue Carbon: Toward an Improved Understanding of the Role of Vegetated Coastal Habitats in Sequestering CO 2."

Frontiers in Ecology and the Environment. doi:10.1890/110004.

[34] Misbari, Syarifuddin, and Mazlan Hashim. 2016. “Change Detection of Submerged Seagrass Biomass in Shallow Coastalwater.” Remote Sensing 8 (3). MDPI AG. doi:10.3390/rs8030200.

[35] Nguyen, Van Tien. 2004. “National Report on Seagrass in the South China Sea - Viet Nam.” Seagrass in the South China Sea.

[36] Nguyen, Van Tien. 2008. “Seagrass in the South China Sea.” National Report, 33.

[37] Nguyen, Van Tien. 2013. “Nguon Loi Tham Co Bien Viet Nam [Seagrass Resources of Viet Nam].” Ha Noi: Nha Xuat Ban Khoa Hoc Tu Nhien va Cong Nghe.

[38] Pham, Thi Thuy Hanh, and Masahide Furukawa. 2007. “Impact of Sea Level Rise on Coastal Zone of Vietnam.” Bulletin of Faculty of Science, University of the Ryukyus 84 (84). 琉球大学理学部: 45–59. https://u-ryukyu.repo.nii.ac.jp/records/2003752.

[39] Pham, Tien Dat, Junshi Xia, Nam Thang Ha, Dieu Tien Bui, Nga Nhu Le, and Wataru Tekeuchi. 2019. “A Review of Remote Sensing Approaches for Monitoring Blue Carbon Ecosystems: Mangroves, Seagrassesand Salt Marshes during 2010−2018.” Sensors (Basel, Switzerland). NLM (Medline). doi:10.3390/s19081933.

[40] Philpot, William. 2007. “Estimating Atmospheric Transmission and Surface Reflectance from a Glint-Contaminated Spectral Image.” IEEE Transactions on Geoscience and Remote Sensing 45 (2): 448–457. doi:10.1109/TGRS.2006.887161.

[41] Phinn, Stuart, Chris Roelfsema, Eva Kovacs, Robert Canto, Mitch Lyons, Megan Saunders, and Paul Maxwell. 2018. Mapping, Monitoring and Modelling Seagrass Using Remote Sensing Techniques. Seagrasses of Australia: Structure, Ecology and Conservation. doi:10.1007/978-3-319-71354-0_15.

[42] Quang, Nguyen Hao, Jun Sasaki, Hiroto Higa, and Nguyen Huu Huan. 2017. “Spatiotemporal Variation of Turbidity Based on Landsat 8 OLI in Cam Ranh Bay and Thuy Trieu Lagoon, Vietnam.” Water (Switzerland) 9 (8). doi:10.3390/w9080570.

[43] Roelfsema, Chris, Eva M. Kovacs, Megan I. Saunders, Stuart Phinn, Mitchell Lyons, and Paul Maxwell. 2013. “Challenges of Remote Sensing for Quantifying Changes in Large Complex Seagrass Environments.” Estuarine, Coastal and Shelf Science 133. Elsevier Ltd: 161–171. doi:10.1016/j.ecss.2013.08.026.

[44] Roelfsema, Chris M., Mitchell Lyons, Eva M. Kovacs, Paul Maxwell,

Megan I. Saunders, Jimena Samper-Villarreal, and Stuart R. Phinn. 2014. “Multi-Temporal Mapping of Seagrass Cover, Species and Biomass: A Semi-Automated Object Based Image Analysis Approach.” Remote Sensing of Environment 150. Elsevier Inc.: 172–187. doi:10.1016/j.rse.2014.05.001.

[45] Sagawa, Tatsuyuki, Etienne Boisnier, Teruhisa Komatsu, Karim ben Mustapha, Abdalla Hattour, Naoko Kosaka, and Sanae Miyazaki. 2010. “Using Bottom Surface Reflectance to Map Coastal Marine Areas: A New Application Method for Lyzenga’s Model.” International Journal of Remote Sensing. doi:10.1080/01431160903154341.

[46] Sani, D. A., and M. Hashim. 2019. “SATELLITE-BASED MAPPING of ABOVE-GROUND BLUE CARBON STORAGE in SEAGRASS HABITAT WITHIN the SHALLOW COASTAL WATER.” International Archives of the Photogrammetry, Remote Sensing and Spatial Information Sciences - ISPRS Archives 42 (4/W16): 587–593. doi:10.5194/isprs-archives-XLII-4-W16-587-2019.

[47] Stumpf, Richard P., Kristine Holderied, and Mark Sinclair. 2003. “Determination of Water Depth with High-Resolution Satellite Imagery over Variable Bottom Types.” Limnology and Oceanography 48 (1part2). John Wiley & Sons, Ltd: 547–556. doi:10.4319/LO.2003.48.1_PART_2.0547.

[48] Sudo, Kenji, T. E.Angela L. Quiros, Anchana Prathep, Cao van Luong, Hsing Juh Lin, Japar Sidik Bujang, Jillian Lean Sim Ooi, et al. 2021. “Distribution, Temporal Change, and Conservation Status of Tropical Seagrass Beds in Southeast Asia: 2000–2020.” Frontiers in Marine Science 8 (July). doi:10.3389/fmars.2021.637722.

[49] Thoai, Duong Thanh, Anh Nguyet Dang, and Nguyen Thi Kim Oanh. 2019. “Analysis of Coastline Change in Relation to Meteorological Conditions and Human Activities in Ca Mau Cape, Viet Nam.” Ocean & Coastal Management 171 (April). Elsevier: 56–65. doi:10.1016/J.OCECOAMAN.2019.01.007.

[50] Thuc, Tran, Nguyen van Thang, Huynh Thi Lan Huong, Mai van Khiem, Nguyen Xuan Hien, Doan Ha Phong, Nguyen van Hiep, et al. 2023. “Climate Change and Sea Level Rise Scenarios for Vietnam.” Coastal-Protection-Mekongdelta.Com. Accessed January 25. http://www.coastal-protection-mekongdelta.com/download/library/136.CC_SLR2016Summary_EN.pdf.

[51] Topouzelis, Konstantinos, Despina Makri, Nikolaos Stoupas, Apostolos Papakonstantinou, and Stelios Katsanevakis. 2018. “Seagrass Mapping in Greek Territorial Waters

Using Landsat-8 Satellite Images." International Journal of Applied Earth Observation and Geoinformation 67 (October 2017). Elsevier: 98–113. doi:10.1016/j.jag.2017.12.013.

[52] Traganos, Dimosthenis, Bharat Aggarwal, Dimitris Poursanidis, Konstantinos Topouzelis, Nektarios Chrysoulakis, and Peter Reinartz. 2018. "Towards Global-Scale Seagrass Mapping and Monitoring Using Sentinel-2 on Google Earth Engine: The Case Study of the Aegean and Ionian Seas." Remote Sensing 10 (8): 1227. doi:10.3390/rs10081227.

[53] Traganos, Dimosthenis, and Peter Reinartz. 2018. "Mapping Mediterranean Seagrasses with Sentinel-2 Imagery." Marine Pollution Bulletin 134 (March). Elsevier: 197–209. doi:10.1016/j.marpolbul.2017.06.075.

[54] Unsworth, Richard K. F., Len J. McKenzie, Catherine J. Collier, Leanne C. Cullen-Unsworth, Carlos M. Duarte, Johan S. Eklöf, Jessie C. Jarvis, Benjamin L. Jones, and Lina M. Nordlund. 2019. "Global Challenges for Seagrass Conservation." Ambio 48 (8). Springer Netherlands: 801–815. doi:10.1007/s13280-018-1115-y.

[55] USGS. 2020. "Landsat 8 Collection 1 (C1) Land Surface Reflectance Code (LaSRC) Product Guide" 1 (August).

[56] Veettil, Bijeesh Kozhikkodan, Raymond D. Ward, Nguyen Thi Kim Dung, Dong Doan Van, Ngo Xuan Quang, Pham Ngoc Hoai, and Nhat Duc Hoang. 2021. "The Use of Bioshields for Coastal Protection in Vietnam: Current Status and Potential." Regional Studies in Marine Science 47 (September). Elsevier: 101945. doi:10.1016/J.RSMA.2021.101945.

[57] Vo, Trong Thach, Khin Lau, Lawrence M. Liao, and Xuan Vy Nguyen. 2020. "Satellite Image Analysis Reveals Changes in Seagrass Beds at Van Phong Bay, Vietnam during the Last 30 Years." Aquatic Living Resources 33 (May). doi:10.1051/alr/2020005.

[58] Waycott, M., C. M. Duarte, T. J. B. Carruthers, R. J. Orth, W. C. Dennison, S. Olyarnik, A. Calladine, et al. 2009. "Accelerating Loss of Seagrasses across the Globe Threatens Coastal Ecosystems." Proceedings of the National Academy of Sciences 106 (30): 12377–12381. doi:10.1073/pnas.0905620106.

Xu, Hanqiu. 2006. "Modification of Normalised Difference Water Index (NDWI) to Enhance Open Water Features in Remotely Sensed Imagery." International Journal of Remote Sensing 27 (14): 3025–3033. doi:10.1080/01431160600589179.

Supplement Materials

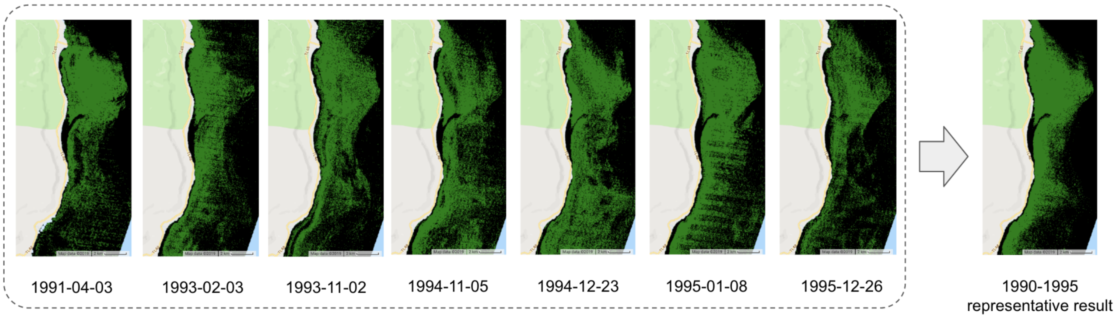

Figure S1: Composition of the mode of classified results in Bai Bon and Bai Vong intertidal flats, Phu Quoc islands.

Table S1: Table of regions in Vietnam, their seagrass species and phenology (Nguyen, 2013).

Region	Species	Phenology
Northeast (Quang Ninh, Hai Phong)	*Zostera japonica, Ruppia maritima, Halodule uninervis, Halophila beccarii, Halophila ovalis, Halophila decipiens*	Density, biomass, and leaf area of Halophila ovalis and Zostera japonica decrease in rainy season (September) and increase in the dry season (December - April)
Red river delta - North Central (from Hai Phong to Hue)	*Zostera japonica, Ruppia maritima, Syringodium isoetifolium*	Grow poorly or die in the rainy season (September-Feb), due to high turbidity, low salinity, or uprooted by typhoons. Grow well in dry season (March-August)
South Central (Da Nang, Quang Nam, Quang Ngai, Binh Dinh, Phu Yen, Khanh Hoa, Ninh Thuan, Binh Thuan)	*Zostera japonica, Halodule uninervis, Thalassia hemprichii, Halophila ovalis, Cymodocea rotundata, Halophila decipiens, Halodule pinifolia*	Grow poorly or die in the rainy season (September-February), due to high turbidity, low salinity, or uprooted by typhoons. Grow well in the dry season (March-August) as salinity increases.

Southeast (Vung Tau) Southwest (Kien Giang)	*Zostera japonica, Halodule uninervis, Thalassia hemprichii, Halophila ovalis, Cymodocea rotundata, Halophila decipiens, Halodule pinifolia*	Grow poorly or die in the rainy season in rainy season (September) high in dry season (March)

Table S2: Accuracy for Landsat visual interpretation against UAV data

		My interpretation		Total (pixels)	PA
		Seagrass	Non-seagrass		
Reference from UAV	Seagrass	126	1	127	**99.21%**
	Non-seagrass	1	25	26	**96.15%**
Total (pixels)		127	26	153	
UA		**99.14%**	**99.21%**		

Table S3: Classification result for each seagrass site in 1985-1990 and 2015-2019 period and the percentage lost

Location	Landsat Scene (Alphabet name - Path, Row)	Area in 1985-1990 period (ha)	Area in 2015-2019 period (ha)	Percentage lost
Lang Co Lagoon	A - 125, 048	240	145	39.54%
Tam Giang - Cau Hai Lagoon	B - 125, 049	8534	2116	75.21%
Han River Estuary	C - 124, 049	310	91	70.70%
Cua Dai Estuary	C - 124, 049	306	44	85.50%
Nui Thanh Lagoon	C - 124, 049	1570	220	86.02%
Thi Nai Lagoon	D - 123, 050	713	362	49.24%
Cu Mong Lagoon	E - 123, 051	806	332	58.85%
Xuan Dai Bay	E - 123, 051	894	249	72.14%
O Loan Lagoon	E - 123, 051	376	238	36.83%
Van Phong Bay	E - 123, 051	3570	716	79.94%
Nha Trang Bay	F - 123, 052	848	254	70.09%
Thuy Trieu	F - 123, 052	682	441	35.31%

Lagoon				
Cam Ranh Bay	F - 123, 052	3387	1326	60.86%
Nha Phu Bay	F - 123, 052	422	66	84.45%
Thai An Tidal flat	F - 123, 052	133	89	33.07%
My Hoa Tidal Flat	F - 123, 052	421	205	51.22%
Nai Lagoon	F - 123, 052	1121	310	72.32%
Vinh Hao Tidal Flat	F - 123, 052	705	239	66.13%
Rach Vem Estuary	G - 126, 053	680	379	44.36%
Bai Bon Tidal Flat	G - 126, 053	3787	4338	-14.53% (increased)
Bai Vong Tidal Flat	G - 126, 053	3672	2870	21.83%
Bai Dam Tidal Flat	G - 126, 053	1114	551	50.53%
Mui Ong Doi Bay	G - 126, 053	220	176	20.17%
Mui Ham Rong Bay	G - 126, 053	389	398	-2.40% (increased)
Bai Trau Nam Tidal flat	G - 126, 053	1284	927	27.76%
Total		36185	17081	52.79%

Table S4. Table of seagrass sites that could not be identified in our analysis, with area according to literature survey (Cao et al., 2012; Nguyen, 2013)

Site name	Area range (hectare)
De Gi Lagoon	50 - 50
Han River	30 - 300
Cua Dai Estuary	160 - 375
Thu Bon estuary	50 - 50
Dinh Vu	30 - 120
Lach Huyen	0 - 60
Trang Cat	2 - 60
Cat Hai lagoon	60 - 100
Nha Mac lagoon	240 - 500
Gia Luan	0 - 100
Ha Long Bay	30 - 30
Hà Cối	5 - 150
Quan Lan tidal flat	2 - 100
Ha Lagoon	3 - 80
Ngan Sanddune	0 - 30
Kim Trung	60 - 120
Dong Long	150 - 150

Thanh Long	80 - 80
Xuan Hoi	50 - 50
Nhat Le - Dong Hoi	80 - 200
Gianh River	250 - 500
Lo River	6 - 8
Van Gia	0 - 10
Cua Be River	1 - 10
Hon Bip	0 - 10
Vung Bau	0 - 200
Ha Rong lagoon	100 - 200
Vu Yen lagoon	15 - 20
Thuy Nguyen lagoon	10 - 15
Hai Hau	190 - 240
Buon Lagoon	0 - 100
Total	**1654 - 4018**